hv photonics

IMPACT FACTOR 2.1

CITESCORE 2.6

Article

Novel Application of Quantum Computing for Routing and Spectrum Assignment in Flexi-Grid Optical Networks

Oumayma Bouchmal, Bruno Cimoli, Ripalta Stabile, Juan Jose Vegas Olmos, Carlos Hernandez, Ricardo Martinez, Ramon Casellas and Idelfonso Tafur Monroy

Special Issue

Optical Communication Networks: Advancements and Future Directions

Edited by

Dr. Shu-Hao Chang and Dr. Chin-Yuan Fan

MDPI

https://doi.org/10.3390/photonics11111023

photonics

MDPI

Article

Novel Application of Quantum Computing for Routing and Spectrum Assignment in Flexi-Grid Optical Networks

Oumayma Bouchmal [1,*], Bruno Cimoli [1], Ripalta Stabile [1], Juan Jose Vegas Olmos [2], Carlos Hernandez [3], Ricardo Martinez [3], Ramon Casellas [3] and Idelfonso Tafur Monroy [1]

[1] Department of Electrical Engineering, Eindhoven University of Technology (TU/e), 5612 AZ Eindhoven, The Netherlands; b.cimoli@tue.nl (B.C.); r.stabile@tue.nl (R.S.); i.tafur.monroy@tue.nl (I.T.M.)
[2] NVIDIA Corporation, Yokneam Illit 2066730, Israel; juanj@nvidia.com
[3] Centre Tecnològic de Telecomunicacions de Catalunya (CTTC-CERCA), 08860 Castelldefels, Spain; chernandez@cttc.es (C.H.); ricardo.martinez@cttc.es (R.M.); ramon.casellas@cttc.es (R.C.)
* Correspondence: o.bouchmal@tue.nl

Abstract: Flexi-grid technology has revolutionized optical networking by enabling Elastic Optical Networks (EONs) that offer greater flexibility and dynamism compared to traditional fixed-grid systems. As data traffic continues to grow exponentially, the need for efficient and scalable solutions to the routing and spectrum assignment (RSA) problem in EONs becomes increasingly critical. The RSA problem, being NP-Hard, requires solutions that can simultaneously address both spatial routing and spectrum allocation. This paper proposes a novel quantum-based approach to solving the RSA problem. By formulating the problem as a Quadratic Unconstrained Binary Optimization (QUBO) model, we employ the Quantum Approximate Optimization Algorithm (QAOA) to effectively solve it. Our approach is specifically designed to minimize end-to-end delay while satisfying the continuity and contiguity constraints of frequency slots. Simulations conducted using the Qiskit framework and IBM-QASM simulator validate the effectiveness of our method. We applied the QAOA-based RSA approach to small network topology, where the number of nodes and frequency slots was constrained by the limited qubit count on current quantum simulator. In this small network, the algorithm successfully converged to an optimal solution in less than 30 iterations, with a total runtime of approximately 10.7 s with an accuracy of 78.8%. Additionally, we conducted a comparative analysis between QAOA, integer linear programming, and deep reinforcement learning methods to evaluate the performance of the quantum-based approach relative to classical techniques. This work lays the foundation for future exploration of quantum computing in solving large-scale RSA problems in EONs, with the prospect of achieving quantum advantage as quantum technology continues to advance.

Keywords: flexi-grid; elastic optical networks; routing and spectrum assignment; quantumcomputing; quantum approximate optimization algorithm; quadratic unconstrained binary optimization; quantum optimization

check for updates

Citation: Bouchmal, O.; Cimoli, B.; Stabile, R.; Vegas Olmos, J.J.; Hernandez, C.; Martinez, R.; Casellas, R.; Tafur Monroy, I. Novel Application of Quantum Computing for Routing and Spectrum Assignment in Flexi-Grid Optical Networks. *Photonics* **2024**, *11*, 1023. https://doi.org/10.3390/photonics11111023

Received: 27 September 2024
Revised: 21 October 2024
Accepted: 28 October 2024
Published: 30 October 2024

Copyright: © 2024 by the authors. Licensee MDPI, Basel, Switzerland. This article is an open access article distributed under the terms and conditions of the Creative Commons Attribution (CC BY) license (https://creativecommons.org/licenses/by/4.0/).

1. Introduction

Elastic Optical Networks (EONs) represent a significant advancement in optical communications, offering dynamic and flexible spectrum management that exceeds the capabilities of traditional fixed-grid systems. EONs employ advanced techniques, such as flex-grid technology, adaptive modulation formats, and spectrum slicing, which enable precise allocation of spectrum resources, finely tuning them to meet the diverse demands of different types of data traffic. This high level of adaptability enhances network customization and efficiency, while also reducing unnecessary resource use. Furthermore, the ability of EONs to reconfigure the network in real-time supports enhanced resilience and scalability, making them particularly well suited for the demands of next-generation

networks, including 5G and beyond [1]. As the volume of data traffic continues to grow exponentially, driven by the widespread of IoT devices, cloud computing, and multimedia streaming, the need for such a flexible and robust optical network infrastructure becomes increasingly critical. EONs' capacity to efficiently handle varying traffic loads is essential in meeting the escalating demands of data-driven services, ensuring seamless connectivity and optimized performance across diverse network environments [2].

The effectiveness of EONs relies on solving the routing and spectrum assignment (RSA) problem. RSA involves finding a valid spatial path (i.e., nodes and links) along with a feasible spectral selection (i.e., frequency slot) while dynamically managing and allocating the optical spectrum. A frequency slot (FS) is formed by a central frequency and a slot width. The process of allocating the necessary spectrum must fulfill the continuity and contiguity constraints to establish an end-to-end connection. If a continuous and contiguous FS cannot be found across the entire lightpath, the connection cannot be established [3]. Additionally, optical connection services set specific end-to-end Quality of Service (QoS) requirements, which include guaranteed bandwidth and a maximum permitted end-to-end latency. Consequently, RSA algorithms must satisfy these requirements.

In recent years, machine learning (ML) techniques, particularly deep reinforcement learning (DRL), along with integer linear programming (ILP), have gained prominence as methods to optimize RSA in EONs [4–8]. These approaches offer promising solutions for dynamic and complex network environments. However, they face significant challenges that prevent their effectiveness, especially as optical networks evolve to meet the exponential growth in data traffic and the strict QoS requirements. One of the major limitations of ILP models is their computational complexity, which scales poorly with the network size [9]. As the network expands, the number of potential routing paths and FSs increase exponentially, leading to impractically long solution times for large-scale problems. This issue becomes more grave due to the fact that ILP models often require the formulation of the RSA problem with numerous decision variables, each representing possible configurations or routing decisions within the network. As a result, the time and the computational resources needed to solve these models can become prohibitive, making them less feasible for real-time applications.

Similarly, while DRL offers the advantage of learning and adapting to network conditions over time, it comes with its challenges. Training DRL models is not only time-intensive but also prone to inefficiencies as the network grows. The observation space, which includes all possible states the network can occupy, expands with the network size, leading to what is known as the curse of dimensionality [10]. This phenomenon makes it increasingly difficult for DRL models to converge to an optimal solution within a reasonable time frame. Moreover, the exploration–exploitation trade-off in DRL can result in sub-optimal decision-making during the learning process, potentially degrading network performance, especially in dynamic environments where conditions change rapidly [11,12].

Another limitation of both the ILP and DRL approaches is their difficulty in adapting to real-time changes in network traffic patterns. ILP models, due to their static nature, struggle to integrate dynamic traffic variations without significant recalculations, which are time-consuming. DRL models, on the other hand, may require retraining or fine-tuning to accommodate new traffic patterns or network configurations, which can be impractical in fast-changing environments. These limitations impose the need to explore more advanced techniques for RSA in modern communication in general and EONs in particular.

Quantum computing (QC) emerges as a strong candidate for addressing these challenges, particularly because the RSA problem is proven to be NP-Hard [13]. QC-based techniques leverage properties such as parallelism, superposition, and entanglement, enabling them to solve complex optimization problems that are infeasible for classical techniques [14]. By combining machine learning (ML) techniques with the unique features of QC, a new framework known as quantum machine learning (QML) has emerged. QML involves processing classical data on a quantum computer using ML algorithms, a process known as quantum encoding [15]. Since its introduction, QML has demonstrated the potential to

significantly reduce the time complexity and learning process for many computationally intense operations, including those in 6G applications. Several studies have proposed QML as a key technology for solving hard optimization problems, offering a promising approach to NP-Hard challenges like RSA [16,17].

In this context, QC-based techniques will provide a fundamentally different approach to address the complexities of the RSA problem by leveraging quantum parallelism and entanglement. Unlike classical algorithms that must evaluate potential solutions sequentially, QC can process multiple possibilities simultaneously, significantly reducing the time needed to solve large and complex optimization problems. This ability to explore a vast solution space in parallel makes QC particularly advantageous for problems like RSA, where both routing and spectrum assignment must be optimized under strict constraints. Furthermore, the potential of QC for scalability offers an effective direction to address the growing demands of next-generation optical networks, enabling faster, more efficient resource allocation in dynamic large-scale environments. In light of this, in this paper, we propose a novel quantum-based solution for the RSA problem in EONs, aimed at minimizing end-to-end delay while considering the continuity and contiguity constraints of the selected FSs. To the best of the authors knowledge, this is the first work to apply a QC method to solve the RSA problem in EONs.

The rest of this paper is organized as follow: Section 2 gives an overview of QC and how to use it to solve an optimization problem. Section 3, provides a detailed explanation of the process followed to solve the RSA problem using QC-based technique including the network modeling, the mathematical formulations, and the mapping process. In Section 4, we present the results obtained and a comparative analysis of QAOA, ILP, and DRL. Finally, Section 5 summarizes and concludes the article.

2. Background and Methodology

This section outlines the key concepts and recent advancements in QC relevant to this work. We first discuss the principles and challenges of Noisy Intermediate-Scale Quantum (NISQ) devices, followed by the role of variational quantum algorithms (VQAs) in the NISQ era and the workflow we need to follow to solve the RSA problem using a VQA algorithm.

2.1. Quantum Computing in the Noisy Intermediate-Scale Quantum Era

Quantum computing (QC) uses the principles of quantum mechanics, a fundamental branch of physics that describes the behavior of matter and energy on very small scales. In classical computing, the basic unit of information is a bit, which can be either 0 or 1. QC, however, uses quantum bits (qubits) that can exist in a state of 0, 1, or both simultaneously, a property known as superposition. Additionally, qubits can be entangled, meaning the state of one qubit is directly related to the state of another, no matter how far apart they are. These properties allow quantum computers to perform many calculations at once—a phenomenon known as quantum parallelism—potentially solving certain complex problems much faster than classical computers [18].

In 2016, the first cloud-based quantum computer was made accessible to the public [19]. Yet, noise and limitations in qubit performance constrained significant implementations and problem-solving. However, interest and excitement grew around the potential of these devices, which have been called Noisy Intermediate-Scale Quantum (NISQ) computers [20]. Today's state-of-the-art quantum devices, which range in size from 50 to 1200 qubits, have demonstrated the ability to achieve "quantum supremacy"—outperforming the most advanced classical supercomputers on specific, carefully designed mathematical tasks [21,22]. However, the full potential of QC, particularly in providing speedups for practical applications—a milestone referred to as "quantum advantage" has yet to be fully realized. Additionally, the development of fault-tolerant quantum computers, which are essential for broader and more reliable applications, is still a work in progress. A critical technological question is how to best leverage today's NISQ devices to achieve quantum advantage. Any effective strategy must consider the limitations of these devices, including

the limited number of qubits, restricted qubit connectivity, and the presence of both coherent and incoherent errors that constrain the depth of quantum circuits.

Variational quantum algorithms (VQAs) have emerged as the most promising approach to achieving quantum advantage on NISQ devices. They are designed to run on gate-based quantum computers to solve complex optimization problems. VQAs involve both quantum and classical processors. the quantum part contains a variational quantum circuit, also known as the Ansatz, where the parameters are tunable variables. These circuits are designed to approximate the solution to a given optimization problem. After the circuit is executed and results are obtained, a classical optimizer is used to adjust and update the parameters to improve the outcome iteratively [23], as depicted in Figure 1.

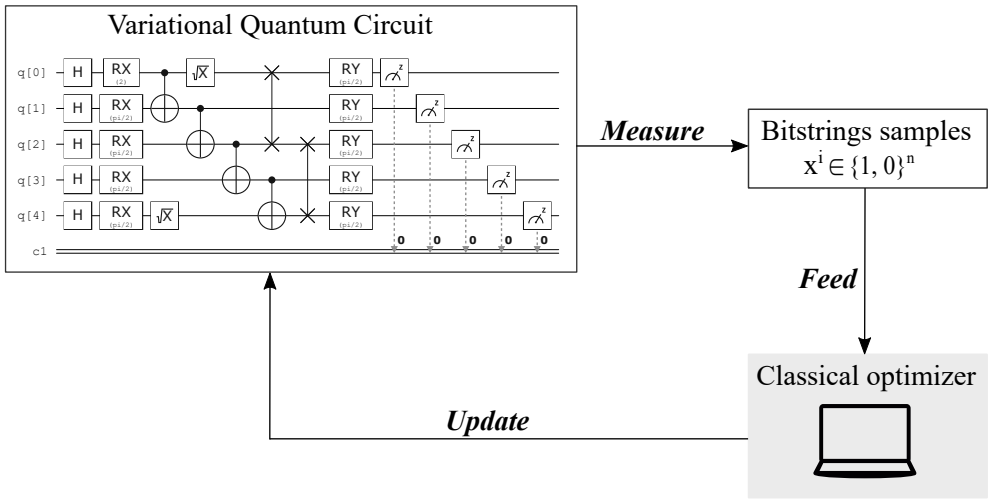

Figure 1. Hybrid quantum–classical loop of variational quantum algorithms.

What makes VQAs particularly well suited for NISQ devices is their relative robustness to noise. By keeping quantum circuits relatively shallow and offloading part of the computational workload to classical processors, VQAs can work effectively even on quantum computers that are not yet fully fault-tolerant. In this regard, several studies have adopted VQAs to enhance different aspects of quantum machine learning such as quantum neural networks [24,25], quantum kernel methods [26,27] and quantum federated learning [28,29].

2.2. Solving Optimization Problems Using Gate-Based Quantum Computers

In the field of quantum optimization, solving an optimization problem using VQAs often involves mapping the problem onto a gate-based quantum system, where the optimal solution corresponds to the system's ground energy state—the lowest energy configuration. One of the most popular algorithms used for this purpose is the Quantum Approximate Optimization Algorithm (QAOA). QAOA encodes the optimization problem into a Hamiltonian, which represents the total energy of the system in quantum terms. Following the hybrid loop presented in Figure 1, the algorithm employs a variational quantum circuit to approximate the ground state of this Hamiltonian, the components of this circuit are depicted in Figure 2. The green layers correspond to the application of the cost Hamiltonian H_c which encodes the problem to be optimized. These layers are responsible for introducing phase shifts proportional to the cost function values and they are characterized by parameter γ. The pink layers correspond to the application of the mixing Hamiltonian H_B, which facilitates the exploration of the solution space by applying rotations that expand the search space of the algorithm and they are characterized by parameter β. Afterward, the circuit parameters are iteratively updated through a classical optimizer until the combination that minimizes the energy is found.

Returning to our objective, the key elements of the process we follow in this work to solve the RSA problem using QAOA are depicted in Figure 3. The first step in the process is

the *Input Stage*, where the user provides the network topology, a fully defined mathematical formulation of the problem—including the cost function, the available spectrum slots, and the requirements of a traffic demand R_i.

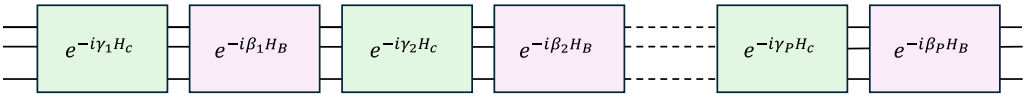

Figure 2. The key components of the QAOA variational circuit.

After defining the optimization problem, the second step is the *Mapping Stage*. As mentioned previously, solving an optimization problem using QAOA involves mapping it to gate-based quantum hardware. One technique to achieve this is by formulating the problem as a Quadratic Unconstrained Binary Optimization (QUBO) problem. QUBO is a widely used mathematical model for representing a range of combinatorial optimization problems [30]. *Quadratic* refers to the fact that the cost function must be quadratic, while *binary* indicates that the variables can only take values of 0 or 1.

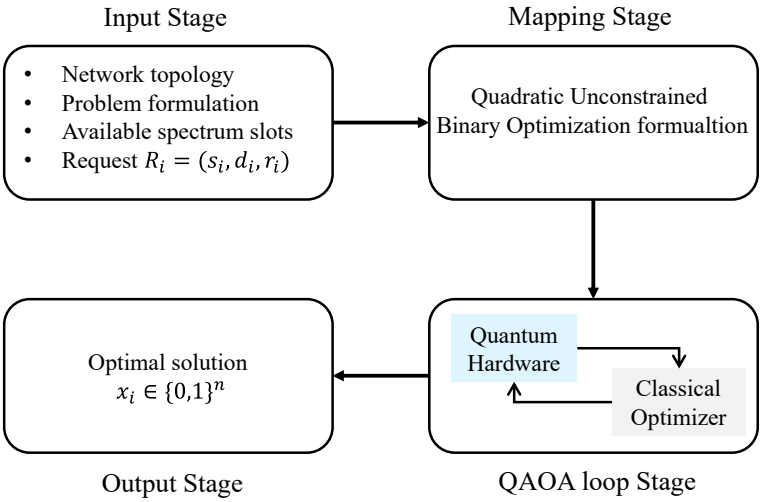

Figure 3. Workflow of the QAOA-based approach used to solve the RSA problem in this study.

In the *QAOA Loop Stage*, the variational quantum circuit is executed on the quantum hardware, and its parameters are iteratively updated using a classical optimizer. This loop is repeated until the ground state energy of the system is found. Finally, in the *Output Stage*, the solution to the RSA problem is returned to the user.

3. QAOA Applied to Routing and Spectrum Assignment in EONS

In this section, we will provide a detailed explanation of the mathematical formulation of the RSA problem and the mapping process used to solving it using the QAOA. We will follow the process outlined in Figure 3, starting with the network topology and problem formulation, and proceeding through the stages of mapping the problem onto a quantum system, executing the QAOA, and interpreting the results.

3.1. Network Modeling

An EON is modeled as a directed graph $G = (V, E)$, where V represents the set of nodes (i.e., optical switches, or ROADMs) and E the set of optical links (i.e., single-mode optical fibers). We define $s_{i,j}^m$ as the set of basic FSs or slices that can be allocated in each fiber link within E and $d_{i,j}$ the delay between nodes i and j, and $m \in \{1, 2, \ldots, M\}$ represents the number of spectrum slots on each edge. As shown in Figure 4, in this model blue indicates the availability of a slot, whereas red signifies that the slot is occupied, thus it cannot be allocated. Additionally, we define R as the set of traffic demand with each demand R_i

characterized by a tuple (s_i, d_i, r_i), where s_i is the source, d_i is the destination and r_i is the requested number of individual spectrum slot (i.e., frequency slot size).

In this work, we are considering contentionless, directionless, and colorless ROADMS (CDC) with transparent optical networks in the sense that there are continuity and contiguity constraints. Nodes have unlimited ingress and egress destinations, and we have no constraint on the number of internal ports. The links are assumed homogeneous with standard single-mode fibers and we are considering a reduced number of slots (five frequency slots per link) for practical reasons, which would correspond to using only the C band.

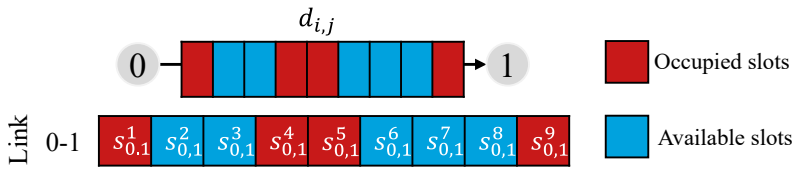

Figure 4. Example of constraints used for RSA with optical link delays.

3.2. Problem Formulation of RSA

The RSA problem consists of two sub-problems: The routing problem, where we need to select for each traffic demand a path through the optical network. The spectrum assignment problem where we need to assign for each demand an interval of consecutive FSs, known as the channel, such that the intervals of lightpaths using the same edge are disjoint. In this regard, the mathematical formulation of the RSA including all these constraints is as follows:

- Decision Variables:

$$x^m_{i,j} = \begin{cases} 1 & \text{if slot } m \text{ is allocated on link } (i,j) \\ 0 & \text{otherwise} \end{cases} \tag{1}$$

- Spectrum capacity (uniqueness constraint): a slot in a link can be allocated to one request at most, defined by

$$s^m_{i,j} = \begin{cases} 1 & \text{if a slot } m \text{ is available} \\ 0 & \text{otherwise} \end{cases} \tag{2}$$

- The objective function:

$$H_o = \min \sum_{i,j,m} d_{ij} x^m_{ij} s^m_{i,j} \tag{3}$$

- Flow conservation: this includes source constraint (ensure that the source node has more outgoing than incoming edges), destination constraint (ensure that the destination node has more incoming than outgoing edges), and path connectivity constraint (ensure that the selected path is connected), formulated as follows:

$$\begin{cases} H_s = \sum_j x^m_{i,j} s^m_{i,j} - 1, \text{if } i = \text{src} \\ H_d = \sum_k x^m_{k,i} s^m_{k,i} - 1, \text{if } i = \text{dst} \\ H_p = \sum_{i \notin s,d} \left(\sum_j x^m_{i,j} s^m_{i,j} - \sum_k x^m_{k,i} s^m_{k,i} \right) \end{cases} \tag{4}$$

- Spectrum contiguity: for each request, the slots should be allocated next to each other, represented by

$$H_{\text{slots}} = \sum_{m=1}^{r_i} \left(\sum_{i,j} x^m_{i,j} s^m_{i,j} - \sum_{j,k} x^m_{j,k} s^m_{j,k} \right) \tag{5}$$

- Spectrum continuity: for each request, the subset of allocated slots should be the same for each link on the selected routing path. This constraint is achieved by fulfilling Equations (2) and (4).
- Allocating the needed slot: for each request, exactly r_i slots need to be allocated, formulated as

$$H_{r_i} = \sum_{m=1}^{M} x_{i,j}^{m} s_{i,j}^{m} - r_i \tag{6}$$

3.3. Mapping Process: Quadratic Unconstrained Binary Optimization Formulation (QUBO)

Following the process described in Figure 3, we will use the QUBO formulation to map the RSA problem onto a gate-based quantum computer. The mathematical formulation of the QUBO problem is as follows:

$$\begin{aligned} &\text{Minimize} \quad X^T Q X + C^T X \\ &\text{subject to} \quad X \in \{0,1\}^n,\ Q \in \mathbb{R}^{n \times n},\ \text{and } C \in \mathbb{R}^n \end{aligned} \tag{7}$$

In this formula, the matrix Q represents the quadratic part of the problem, while the vector C represents the linear part. The goal is to find the vector X that minimizes the entire expression $X^T Q X + C^T X$ under the constraint that X is a binary vector, meaning each element of X belongs to the set $0, 1$.

To reformulate the mathematical problem presented in the previous section as a QUBO, we need to apply a quadratic transformation to all the constraints. This transformation allows us to construct and extract the Q matrix.

- Decision variables: in this case, the decision variable will be the vector X, which we aim to find. For consistency, we will denote the variable as $X_{i,j}^{m}$.
- Flow conservation:

$$\begin{cases} H_s = \left(\sum_j X_{i,j}^{m} s_{i,j}^{m} - 1\right)^2, \text{if } i = \text{src} \\ H_d = \left(\sum_k X_{k,i}^{m} s_{k,i}^{m} - 1\right)^2, \text{if } i = \text{dst} \\ H_p = \sum_{i \notin s,d} \left(\sum_j X_{i,j}^{m} s_{i,j}^{m} - \sum_k X_{k,i}^{m} s_{k,i}^{m}\right)^2 \end{cases} \tag{8}$$

- Spectrum contiguity:

$$H_{\text{slots}} = \sum_{m=1}^{r_i} \left(\sum_{i,j} X_{i,j}^{m} s_{i,j}^{m} - \sum_{j,k} X_{j,k}^{m} s_{j,k}^{m} \right)^2 \tag{9}$$

- Allocating the needed slot:

$$H_{r_i} = \left(\sum_{m=1}^{M} X_{i,j}^{m} s_{i,j}^{m} - r_i \right)^2 \tag{10}$$

The total cost function of the RSA problem can be represented as

$$\begin{aligned} H_c = P\left(\sum_j X_{i,j}^{m} s_{i,j}^{m} - 1\right)^2 + P\left(\sum_k X_{k,i}^{m} s_{k,i}^{m} - 1\right)^2 + P \sum_{i \notin s,d} \left(\sum_j X_{i,j}^{m} s_{i,j}^{m} - \sum_k X_{k,i}^{m} s_{k,i}^{m}\right)^2 \\ P' \sum_{m=1}^{r_i} \left(\sum_{i,j} X_{i,j}^{m} s_{i,j}^{m} - \sum_{j,k} X_{j,k}^{m} s_{j,k}^{m} \right)^2 + P'' \left(\sum_{m=1}^{M} X_{i,j}^{m} s_{i,j}^{m} - r_i \right)^2 + \sum_{i,j,m} d_{ij} X_{ij}^{m} s_{i,j}^{m} \end{aligned} \tag{11}$$

With P, P' and P'' as penalty coefficients to enforce constraint compliance.

With some reordering and grouping alike terms together, we recognized the required form $XQX^T + C^TX$, where the quadratic part (Q matrix), the linear part (the C vector) and the QUBO variables is given by

$$Q = \begin{pmatrix} Q^1_{0,1} & Q^2_{0,1} & Q^3_{0,3} & \cdots & Q^{M-1}_{j,D} & Q^M_{j,D} \\ 0 & Q^1_{0,2} & Q^2_{0,2} & \cdots & Q^{M-1}_{2,i} & Q^M_{2,D} \\ 0 & 0 & Q^1_{1,3} & \cdots & Q^{M-1}_{1,i} & Q^M_{1,D} \\ \vdots & \vdots & \vdots & \ddots & \vdots & \vdots \\ 0 & 0 & 0 & \cdots & Q^{M-1}_{j,j} & Q^M_{j,D} \\ 0 & 0 & 0 & \cdots & 0 & Q^M_{j,D} \end{pmatrix}, X^T = \begin{bmatrix} X^1_{0,1} \\ X^2_{0,1} \\ X^3_{0,1} \\ X^4_{0,1} \\ \vdots \\ X^{M-1}_{j,D} \\ X^M_{j,D} \end{bmatrix}, \quad C^T = \begin{bmatrix} c^1_{0,1} \\ c^2_{0,1} \\ c^3_{0,1} \\ c^4_{0,1} \\ \vdots \\ c^{M-1}_{j,D} \\ c^M_{j,D} \end{bmatrix} \tag{12}$$

The matrix Q is of size $K \times K$, and both the vectors X and C have a length of K with

$$K = \text{Total number of FSs in the network} - \text{Number of occupied FSs} \tag{13}$$

3.4. Equivalent QAOA Ansatz

Going back to our objective, which is mapping the RSA problem to gate-based quantum computer and solve it using the QAOA, Figure 5 show the part of the Ansatz used in the process.

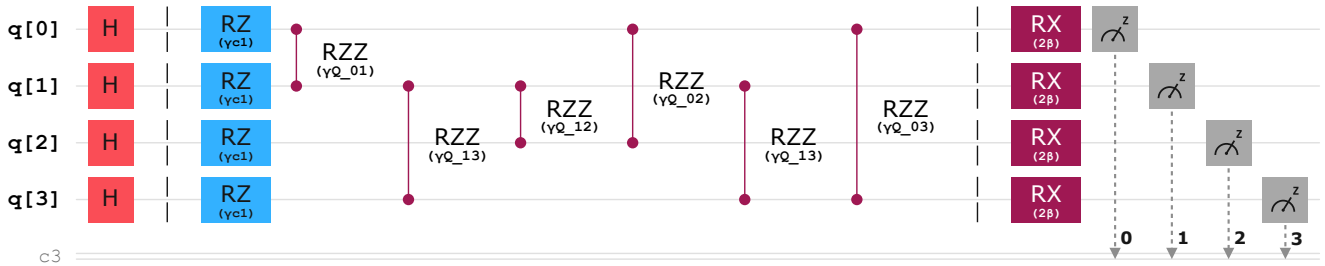

Figure 5. The QAOA Ansatz circuit used in this paper, where each qubit corresponds to an available FS in the network.

The qubits in the circuit represent the available FSs in the network. The first layer of the circuit applies Hadamard gates to all qubits, putting them in an equal superposition. The second layer corresponds to the cost Hamiltonian discussed previously. This layer consists of two types of gates: the first are the R_z gates, which encode the linear part of the QUBO formula (i.e., the C vector). R_z are single-qubit gates that apply a rotation around the z-axis by an angle of γc_i. The second are the R_{zz} gates, which encode the quadratic part of the QUBO (e.g., the Q matrix). R_{zz} are two-qubit gates that represent the interactions between qubits and apply a phase shift around the z-axis by an angle $\gamma Q_{i,j}$. The final layer is the mixer Hamiltonian, which consists of R_x gates. These gates are single-qubit gates that apply a rotation around the x-axis by an angle 2β.

Typically, the number of Hadamard, R_z, and R_x gates is proportional to the number of qubits (i.e., the number of available FSs). However, the number of R_{zz} gates depends on the number of non-zero values in the Q matrix. For clarity and space efficiency, the circuit shown here represents a scenario with four available frequency slots. In practice, for a network with M available FSs, the circuit would include M qubits, M Hadamard, R_z, and R_x gates, while the number of R_{zz} gates would be determined by the specific structure of the Q matrix.

4. Simulation Results and Discussion

In this section, we present the case study and the results obtained from our simulations. To evaluate the feasibility of the proposed QC-based approach for solving the RSA problem, we conducted a comparative analysis against two classical methods: ILP and DRL. By comparing solution quality, time-to-solution, scalability, and real-time adaptability, we highlight both the strengths and limitations of the QC-based approach in comparison to these well-established techniques.

4.1. Case Study and Implementation

We conducted simulations on different graphs to validate and study the performance of the proposed QAOA approach in RSA. These simulations were executed using the Qiskit framework and the IBM-QASM quantum simulator (32 qubits). To update the VQC parameters, we used the Constrained Optimization BY Linear Approximation (COBYLA) optimizer. For results visualization and due to qubits limitations, we present the outcomes from the graph in Figure 6. In our simulation, we have $m \in \{1, 2, \ldots, M\}$ representing the number of FSs available on each edge which is in this case 5 and $K = 10$. We evaluated a scenario where the request $R_i = (0, 3, 2)$ involves sending data from node 0 to node 3, with the requirement of allocating two continuous and contiguous spectrum slots. To maintain the constraints, we tuned the penalties to $P = P' = 40$ and $P'' = 100$.

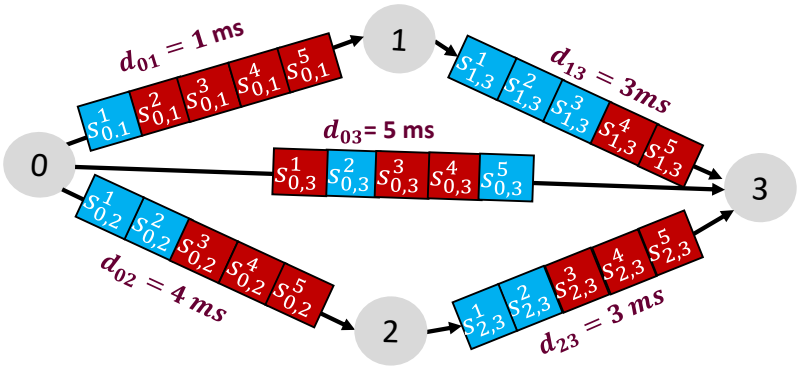

Figure 6. An example of the graph used for the simulation.

As mentioned previously, the angle β in QAOA controls the application of the *mixing Hamiltonian*, which facilitates the algorithm's *exploration of the solution space*. This part of the algorithm allows the quantum state to move across different configurations—in this case, different *routing paths* and *spectrum assignments*. By tuning β, we ensure that the quantum system continues exploring these configurations, helping to avoid becoming trapped in *local minima*. The angle γ in QAOA controls the application of the *problem Hamiltonian*, which guides the algorithm's focus toward *minimizing the QUBO function*. In the context of our problem, this part of the algorithm helps the quantum system to favor configurations that lead to *better routing paths and spectrum assignments*, thereby driving the system toward *lower energy states*. By tuning γ, we direct the quantum state to prioritize solutions that minimize the objective, ultimately pushing the system closer to the optimal solution. Thus, the best combination of β and γ is the one that balances *exploration* and *exploitation*, guiding the quantum circuit toward finding the optimal configuration of routes that minimizes the QUBO cost function [31].

Following this logic, we began the loop with $[\beta, \gamma] = [0.0, 0.0]$ then we used COBYLA to find the optimal parameters. For the simple graph in Figure 6, it is easy to notice that the optimal solution for the RSA is to allocate the slots $s^1_{0,2}$ and $s^2_{0,2}$ on link $(0, 2)$ and slots $s^1_{2,3}$ and $s^2_{2,3}$ on link $(2, 3)$ with a total delay of 7 ms, which gives the bitstring $|0110000011\rangle$. However, our objective is to validate the proposed approach.

Figures 7 and 8 show the evolution of β and γ values alongside the minimum energy over the first 200 iterations of the QAOA. In both plots, the green curve (for β) and the

orange curve (for γ) represent how these parameters evolve over time, while the blue dashed line in both figures tracks the minimum energy at each iteration.

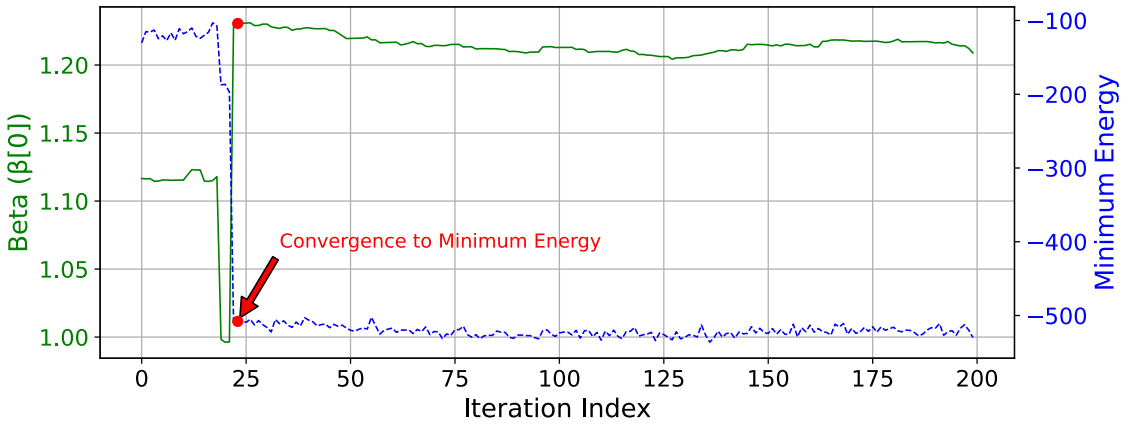

Figure 7. The evolution of β values (in radians) and the corresponding minimum energy over iterations.

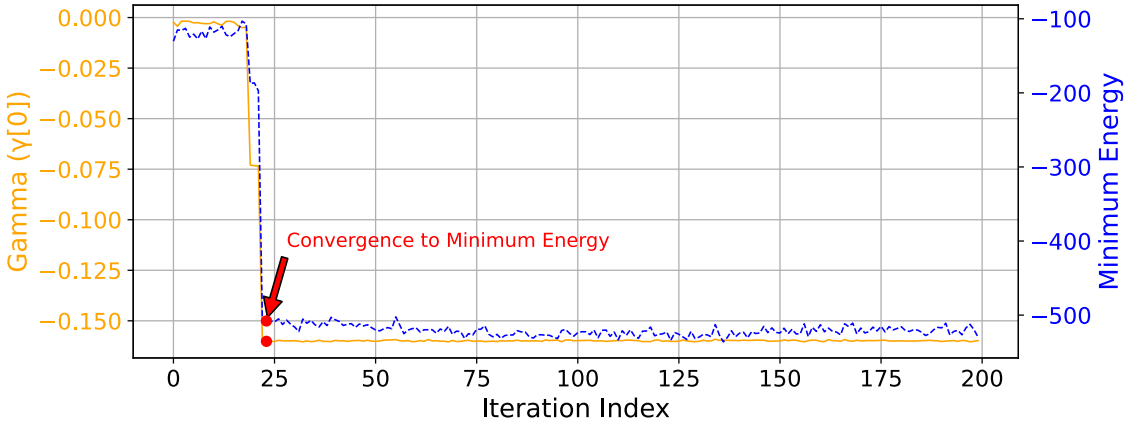

Figure 8. The evolution of γ values (in radians) and the corresponding minimum energy over iterations.

In both plots, a significant drop in energy is observed around iteration 24, annotated as the "Convergence to Minimum Energy". This drop marks the point $[\beta, \gamma] = [1.208778, -0.159569]$ where the algorithm begins to converge toward configurations that result in lower cost (i.e., lowest energy state -556.58325), bringing the system closer to the optimal solution.

As iterations progress, the β and γ values stabilize, indicating that the quantum system has settled into configurations that minimize the QUBO cost function. The flat energy curves beyond iteration 25 in both plots suggest that the system has found near-optimal solutions, and further exploration no longer results in significant improvements.

In general, for an optimization problem with n elements, the solution space is represented by a 2^n dimensional Hilbert space, with each dimension corresponding to a computational basis vector $|X\rangle$. In our context, these elements are the spectrum slots, and for probability distribution analysis, we focus on the top 20 vectors sampled from our final quantum states. Figure 9 illustrates the distribution of these quantum states across various computational basis states (bitstrings). Each bitstring on the y-axis represents a potential combination of spectrum slots that can be allocated within the selected lightpaths. The length of each bar in the diagram indicates the probability of sampling the corresponding bitstring when we sample from our quantum states (x-axis). The objective function values (i.e., energy values) associated with these bitstrings are displayed on the right-hand side. The bar colors represent the energy levels found during the simulation, with yellow indicating higher energy values and purple representing the lowest energy

values. After 24 iterations of the optimization loop, the bitstring $|0110000011\rangle$, which corresponds to the optimal solution, displayed a higher sampling probability of 3.4% compared to the other bitstrings. The entire optimization process was completed efficiently, taking approximately 10.7 s and resulting in a minimum energy of -556.58325.

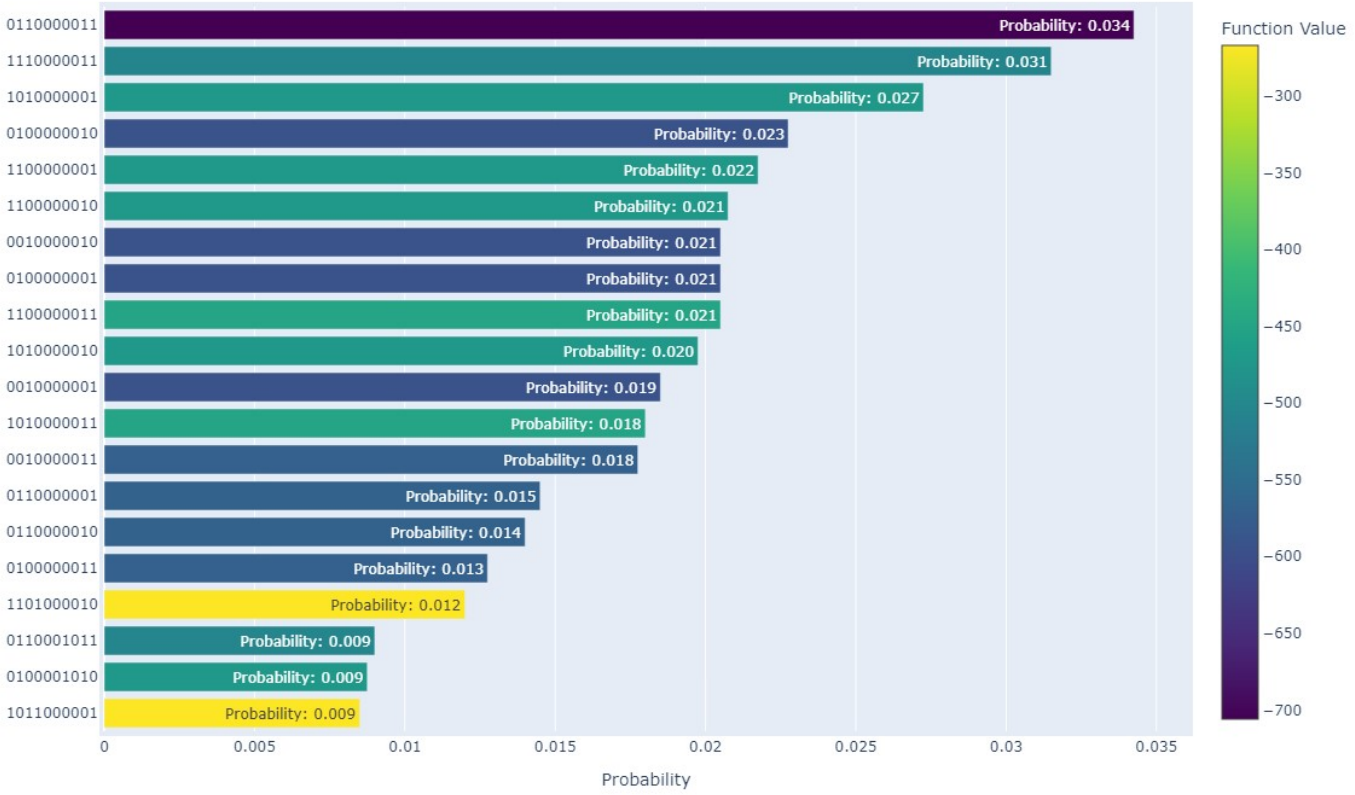

Figure 9. Probability distribution of the possible path solutions and their corresponding energy values.

One of the ways to evaluate the quality of the solution found by any approximation algorithm in general, and the QAOA in particular, is by calculating *the approximation ratio*, which compares the objective value of the solution obtained to the known optimal value as depicted in Equation (14).

$$\text{Approximation Ratio} = \frac{|\text{Objective Value (QAOA)}|}{|\text{Optimal Value}|} = \frac{556.58325}{706} \approx 0.788 \tag{14}$$

The approximation ratio 0.788 indicates that the solution found by the QAOA is approximately 78.8% of the optimal value. While this ratio may not seem particularly close to the optimal in numerical terms, it is important to note that the bitstrings corresponding to the solution found by QAOA match those of the optimal solution. This suggests that the algorithm successfully identified the correct routing paths and spectrum assignments, even if the objective value is not perfectly optimal. The optimal value was calculated using a brute-force classical search, where the algorithm exhaustively evaluated all 1024 (i.e., 2^{10}) possible binary configurations to ensure the exact minimum was found.

The minimum energy, which represents the cost function in the QUBO formulation, is calculated as a weighted sum of the energies of all possible configurations, with the probabilities of each configuration serving as the weights. As a result, the solution is an expectation value that approximates the optimal configuration. By increasing the depth (p) of the QAOA circuit, the algorithm's accuracy can be further improved, allowing the system to explore more configurations in more detail, ultimately yielding solutions that are even closer to the optimal value.

However, in our specific case, the depth was set to $p = 1$, and this proved to be sufficient as the QAOA successfully identified the optimal bitstrings for the routing paths and spectrum assignments. Therefore, increasing the depth further was not necessary. In more complex scenarios or larger network configurations, where the solution space is much more intricate, increasing the depth of QAOA would be more feasible and likely necessary to achieve optimal results.

4.2. Theoretical Resource Estimation and Analysis

In the current state of quantum hardware, our simulations are limited by the available number of qubits and high error rates. Specifically, the number of qubits required for this approach scales with the number of available FSs in the network, which is directly proportional to the size of the network topology. As the network size increases, more qubits will be needed to effectively encode and solve the RSA problem. Currently, NISQ devices with up to 1200 qubits can address relatively small instances of the RSA problem. However, by 2026, the development of more powerful quantum computers with error correction capabilities and up to 100,000 qubits is expected [32]. This advancement will enable tackling larger, real-world instances of the RSA problem, with up to 300 links and 300 FSs per link.

To understand the relative performance of our quantum-based approach, it is important to compare it with the most widely used classical methods applied to solve the RSA problem: ILP and DRL. To rigorously assess the performance of these three methods, we will first provide an overview of how the RSA problem is formulated in each case.

Let us consider a network with N nodes, E edges, and S number of FSs. The most basic ILP model contains two decision variables: **routing decision variable** $x_{i,j}$ indicating whether a specific edge between two nodes is used for a particular connection or not, and a **spectrum assignment variable** $y_{k,i,j}$ indicating whether a slot k is assigned to that edge or not [33]. The main types of constraints in the ILP model are the following. *(A)* Flow conservation constraint: Since it holds for each node, the number of constraints is roughly N^2. *(B)* Spectrum assignment constraint (including continuity, contiguity and interference): These constraints are applied to each edge and FS in the network, so the total number of constraints is $(E\text{x}S)$. This means that

$$\text{Total number of variables} = E + (E\text{x}S) = E(1 + S) \tag{15}$$

$$\text{Total number of constraints} \approx N^2 + (E\text{x}S) \tag{16}$$

In the ILP formulation, the size of the problem grows exponentially as the network size increases. This growth is driven by the increase in both variables and constraints, leading to significant challenges in scalability and time to solution [4,34]. For small networks (e.g., 10–20 nodes, 20–30 edges, 5 FSs), ILP models can find the optimal solution in a reasonable time frame that can take from seconds to minutes [33]. However, for larger networks (e.g., 30+ nodes, 50+ edges, 10+ FSs), the number of variables and constraints grows rapidly and can reach thousands. For example, if we take a network with 50 nodes, 100 edges, and 10 FSs per edge, we will have around 1100 variables and 3500 constraints. Solving the ILP in this case may take hours or even days. Moreover, ILP models are in general not suitable for real-time adaptation. Because any change in the network (e.g., node failure or spectrum reallocation) requires resolving the entire problem from scratch, which takes a long time in large networks.

In DRL, the RSA problem is typically formulated as a Markov Decision Process (MDP) where an agent learns to take actions (routing paths and spectrum assignments) that maximize long-term rewards. Unlike ILP, where the solution is found by directly solving a set of constraints and minimizing a cost function, DRL solves the problem by interacting with the environment and learning the best strategy over time through trial and error. In DRL, the RSA problem can be broken into the following components [35]:

- **State S:** this represents the current state of the network including the network topology information, the spectrum availability distribution (in this part the continuity and contiguity), and the traffic request (number of FSs needed, the source and destination nodes).
- **Action A:** when a traffic request arrives, the DRL agent is to make an action by selecting a routing path and assigning the FSs.
- **Reward Function R(s, a):** the reward function gives feedback to the agent based on the action taken. The goal is to maximize cumulative rewards over time. A typical reward function for the RSA problem might combine multiple objectives, such as maximizing the throughput, minimizing the spectrum usage, the interference, and the latency. A typical reward function could look like the following:

$$R(s,a) = \alpha \cdot R_{\text{throughput}}(s,a) - \beta \cdot R_{\text{spectrum}}(s,a) - \gamma \cdot R_{\text{interference}}(s,a) - \delta \cdot R_{\text{latency}}(s,a)$$

with α, β, γ, and δ are weights that control the relative importance of each objective.
- **Policy $\pi(a|s)$:** the policy is what the DRL model learns—it maps states to actions aiming to maximize the expected cumulative reward.

During training, the DRL model tries different actions (routing paths and spectrum assignments) and receives feedback in the form of rewards. Over time, the model learns to maximize the expected cumulative reward by taking actions that lead to better routing and spectrum assignment decisions.

To better understand the performance of the DRL model, let us consider a network with N nodes, E edges, and S number of FSs. As the network grows, both the **state space** and **action space** increase exponentially. The state space, which includes all possible configurations of the network (spectrum availability, traffic demands, etc.), grows as S^E, meaning for each edge there are S possible spectrum assignments. This results in an exponential number of possible configurations for the agent to explore and learn from during training. Similarly, the action space expands rapidly as the number of possible routing paths between nodes increases with N, and for each selected path, there are S different spectrum allocation options across multiple edges [8,10].

Typically, the solution quality (i.e., optimality) of a well-trained DRL model for solving RSA can approach 90–95% [36]. However, as the state and action spaces expand exponentially with increasing network size, the model must explore a significantly larger number of configurations and decisions. This expansion makes it more challenging for the agent to learn an optimal policy and maintain high solution quality. Moreover, as the network size grows, the training process becomes increasingly time-consuming. While training a basic DRL model on a moderate-sized network (e.g., 10–50 nodes, 20–100 edges, 10–50 FSs) might take several days, larger networks (e.g., 100+ nodes, 1000+ edges, 100+ FSs) could extend the training time to weeks or even months before producing satisfactory results [37].

Table 1 summarizes the key metrics used for this comparison, including solution quality (i.e., the optimality of the path and spectrum slot allocation), time to solution, scalability as network size increases, and adaptability to real-time changes.

Table 1. Comparison of ILP, DRL, and QAOA methods for solving the RSA problem.

Metric	ILP [9,34,38,39]	DRL [12,35–37,40]	This Work (QAOA)
Solution Quality	100% (optimal)	90–95% (near-optimal)	78.8% (can be higher)
Time-to-Solution	Days to weeks for large networks (50+ nodes)	Days to train, but decisions in real-time	Seconds to minutes (limited by quantum hardware)
Scalability with Network size	Poor (exponential growth in variables and constraints)	Good after training	Good
Real-time Adaptability	Poor (requires re-solving for every change)	Moderate to Good (adapts well after training)	Moderate to Good (quantum hardware currently not real-time)

It is important to mention that the true advantage of QC-based techniques, including QAOA, still remains largely theoretical and requires further time and research to materialize in practical large-scale applications. Quantum algorithms are still in their infancy, and although they show promise, their current limitations are primarily due to the immaturity of quantum hardware. Ongoing research is exploring ways to improve qubit coherence, reduce error rates, and develop more effective quantum algorithms. As these technologies advance, we expect to see a gradual but meaningful shift in the applicability of quantum-based methods like QAOA in real-world scenarios [41,42].

5. Conclusions

In this paper, we presented a quantum-based solution for the RSA problem in EONs. Our approach involved formulating the RSA problem as a QUBO model, enabling the use of the QAOA. In our simulations, we tested the QAOA-based RSA approach on a small network topology, where the number of nodes and FSs were constrained by the available qubit count on current quantum simulators (IBM-QASM with 32 qubits). For this small network, the algorithm converged to an optimal solution in under 30 iterations, with a total runtime of approximately 10.7 s and a solution quality of 78.8%.

To better understand the relative performance of our quantum-based approach compared to classical methods, we performed a comparative analysis between the QAOA, ILP, and DRL methods. We concluded that while ILP offers optimal solution quality, it struggles with scalability and real-time adaptability, making it less suitable for larger networks. DRL, though more adaptable and scalable, still requires extensive training. In contrast, QAOA presents promising potential for scalability and time-to-solution due to the inherent parallelism in QC, though its current performance is limited by the maturity of existing quantum hardware.

While QC techniques like QAOA are still in their infancy, this work can be seen as a proof of concept that lays the groundwork for applying QC-based methods to solve complex problems such as RSA in large-scale networks. Ongoing advancements in quantum technology, particularly in areas like qubit coherence and error correction, are expected to improve the performance of quantum algorithms like QAOA, making them viable alternatives to classical methods in the future. In this regard, our work not only demonstrates the feasibility of solving the RSA problem using QAOA but also opens the door for further research and development in applying QC to optical networks.

Author Contributions: Conceptualization, O.B., B.C., R.S., R.C., R.M., C.H., J.J.V.O. and I.T.M.; methodology, O.B.; software, O.B.; validation, O.B., B.C., R.S., R.C., R.M., C.H., J.J.V.O. and I.T.M.; formal analysis, O.B., B.C., R.S., R.C., R.M., C.H., J.J.V.O. and I.T.M.; investigation, O.B., B.C., R.S., R.C., R.M., C.H., J.J.V.O. and I.T.M.; writing—original draft preparation, O.B.; writing—review and editing, O.B., B.C., R.S., R.C., R.M., C.H., J.J.V.O. and I.T.M.; supervision, O.B., B.C., R.S., R.C., R.M., C.H., J.J.V.O. and I.T.M. All authors have read and agreed to the published version of the manuscript.

Funding: This research was partially funded by Marie Skłodowska-Curie IoTalentum project ITN-ETN with grant number 953442, the EU HORIZON-KDT-JU project HICONNECTS with grant number 101097296, the Dutch Ministry of Economic Affairs and Climate Policy (EZK), as part of the Quantum Delta NL program and the EU SNS Project SEASON, Grant Agreement 101096120.

Informed Consent Statement: Not applicable.

Data Availability Statement: There are no relevant datasets presented in this article.

Conflicts of Interest: J.J.V.O. is employed by NVIDIA. The authors declare that the research was conducted in the absence of any commercial or financial relationships that could be construed as a potential conflict of interest.

Abbreviations

The following abbreviations are used in this manuscript:

EONs	Elastic Optical Networks
RSA	Routing and Spectrum Assignment
QC	Quantum Computing
QAOA	Quantum Approximate Optimization Algorithm
QML	Quantum Machine Learning
QUBO	Quadratic Unconstrained Binary Optimization
FS	Frequency Slot
QoS	Quality of Service
ILP	Integer Linear Programming
DRL	Deep Reinforcement Learning
NISQ	Noisy Intermediate-Scale Quantum
VQAs	Variational Quantum Algorithms
COBYLA	Constrained Optimization BY Linear Approximation
IBM-QASM	IBM Quantum Assembler Simulator
MDP	Markov Decision Process

References

1. Jinno, M. Elastic Optical Networking: Roles and Benefits in Beyond 100-Gb/s Era. *J. Light. Technol.* **2017**, *35*, 1116–1124. [CrossRef]
2. Chatterjee, B.; Oki, E. *Elastic Optical Networks: Fundamentals, Design, Control, and Management*; CRC Press: Boca Raton, FL, USA, 2020. [CrossRef]
3. Chatterjee, B.C.; Sarma, N.; Oki, E. Routing and Spectrum Allocation in Elastic Optical Networks: A Tutorial. *IEEE Commun. Surv. Tutor.* **2015**, *17*, 1776–1800. [CrossRef]
4. Wang, J.; Shigeno, M.; Wu, Q. ILP models and improved methods for the problem of routing and spectrum allocation. *Opt. Switch. Netw.* **2022**, *45*, 100675. [CrossRef]
5. Gu, R.; Yang, Z.; Ji, Y. Machine learning for intelligent optical networks: A comprehensive survey. *J. Netw. Comput. Appl.* **2020**, *157*, 102576. [CrossRef]
6. Boutaba, R.; Salahuddin, M.A.; Limam, N.; Ayoubi, S.; Shahriar, N.; Estrada-Solano, F.; Caicedo, O.M. A comprehensive survey on machine learning for networking: Evolution, applications and research opportunities. *J. Internet Serv. Appl.* **2018**, *9*, 16. [CrossRef]
7. Jiao, Y.; Yin, S.; Jin, T.; Liu, L.; Zhao, L.; Huang, S. Reliability-Oriented RSA Combined with Reinforcement Learning in Elastic Optical Networks. In Proceedings of the 2022 20th International Conference on Optical Communications and Networks (ICOCN), Shenzhen, China, 12–15 August 2022; pp. 1–3. [CrossRef]
8. Hernández-Chulde, C.; Casellas, R.; Martínez, R.; Vilalta, R.; Muñoz, R.M. Experimental evaluation of a latency-aware routing and spectrum assignment mechanism based on deep reinforcement learning. *J. Opt. Commun. Netw.* **2023**, *15*, 925–937. [CrossRef]
9. Urbanucci, L. Limits and potentials of Mixed Integer Linear Programming methods for optimization of polygeneration energy systems. *Energy Procedia* **2018**, *148*, 1199–1205 . [CrossRef]
10. Chen, L. Curse of Dimensionality. In *Encyclopedia of Database Systems*; Springer: Boston, MA, USA, 2009; pp. 545–546. [CrossRef]
11. Bouchmal, O.; Cimoli, B.; Stabile, R.; Vegas Olmos, J.J.; Tafur Monroy, I. From classical to quantum machine learning: Survey on routing optimization in 6G software defined networking. *Front. Commun. Netw.* **2023**, *4*, 1220227. [CrossRef]
12. Nguyen, T.T.; Nguyen, N.D.; Nahavandi, S. Deep Reinforcement Learning for Multiagent Systems: A Review of Challenges, Solutions, and Applications. *IEEE Trans. Cybern.* **2020**, *50*, 3826–3839. [CrossRef]
13. Wang, Y.; Cao, X.; Pan, Y. A study of the routing and spectrum allocation in spectrum-sliced Elastic Optical Path networks. In Proceedings of the 2011 Proceedings IEEE INFOCOM, Shanghai, China, 10–15 April 2011; pp. 1503–1511. [CrossRef]
14. Steane, A. Quantum computing. *Rep. Prog. Phys.* **1998**, *61*, 117. [CrossRef]
15. Schuld, M.; Sweke, R.; Meyer, J.J. Effect of data encoding on the expressive power of variational quantum-machine-learning models. *Phys. Rev. A* **2021**, *103*, 032430. [CrossRef]
16. Nawaz, S.J.; Sharma, S.K.; Wyne, S.; Patwary, M.N.; Asaduzzaman, M. Quantum machine learning for 6G communication networks: State-of-the-art and vision for the future. *IEEE Access* **2019**, *7*, 46317–46350. [CrossRef]
17. Zahedinejad, E.; Zaribafiyan, A. Combinatorial optimization on gate model quantum computers: A survey. *arXiv* **2017**, arXiv:1708.05294.
18. Bouchmal, O.; Cimoli, B.; Stabile, R.; Olmos, J.J.V.; Monroy, I.T. Quantum-Inspired Network Optimization in 6G: Opportunities, Challenges and Open Research Directions. In Proceedings of the Distributed Computing and Artificial Intelligence, Special Sessions I, 20th International Conference, Guimaraes, Portugal, 12–14 July 2023; Springer: Cham, Switzerland, 2023. [CrossRef]
19. research, I. IBM Makes Quantum Computing Available on IBM Cloud to Accelerate Innovation. 2016. Available online: https://www.prnewswire.com/news-releases/ibm-makes-quantum-computing-available-on-ibm-cloud-to-accelerate-innovation-300262512.html (accessed on 7 July 2024).
20. Preskill, J. Quantum Computing in the NISQ era and beyond. *Quantum* **2018**, *2*, 79. [CrossRef]

21. Arute, F.; Arya, K.; Babbush, R.; Bacon, D.; Bardin, J.C.; Barends, R.; Biswas, R.; Boixo, S.; Brandao, F.G.; Buell, D.A.; et al. Quantum supremacy using a programmable superconducting processor. *Nature* **2019**, *574*, 505–510. [CrossRef]
22. Zhong, H.S.; Wang, H.; Deng, Y.H.; Chen, M.C.; Peng, L.C.; Luo, Y.H.; Qin, J.; Wu, D.; Ding, X.; Hu, Y.; et al. Quantum computational advantage using photons. *Science* **2020**, *370*, 1460–1463. [CrossRef]
23. Cerezo, M.; Arrasmith, A.; Babbush, R.; Benjamin, S.C.; Endo, S.; Fujii, K.; McClean, J.R.; Mitarai, K.; Yuan, X.; Cincio, L.; et al. Variational quantum algorithms. *Nat. Rev. Phys.* **2021**, *3*, 625–644. [CrossRef]
24. Beer, K.; Bondarenko, D.; Farrelly, T.; Osborne, T.J.; Salzmann, R.; Scheiermann, D.; Wolf, R. Training deep quantum neural networks. *Nat. Commun.* **2020**, *11*, 808. [CrossRef]
25. Abbas, A.; Sutter, D.; Zoufal, C.; Lucchi, A.; Figalli, A.; Woerner, S. The power of quantum neural networks. *Nat. Comput. Sci.* **2021**, *1*, 403–409. [CrossRef]
26. Schuld, M.; Killoran, N. Quantum Machine Learning in Feature Hilbert Spaces. *Phys. Rev. Lett.* **2019**, *122*, 040504. [CrossRef]
27. Jerbi, S.; Fiderer, L.J.; Poulsen Nautrup, H.; Kübler, J.M.; Briegel, H.J.; Dunjko, V. Quantum machine learning beyond kernel methods. *Nat. Commun.* **2023**, *14*, 517. [CrossRef]
28. Chehimi, M.; Saad, W. Quantum Federated Learning with Quantum Data. In Proceedings of the ICASSP 2022—2022 IEEE International Conference on Acoustics, Speech and Signal Processing (ICASSP), Singapore, 22–27 May 2022; pp. 8617–8621. [CrossRef]
29. Song, Y.; Wu, Y.; Wu, S.; Li, D.; Wen, Q.; Qin, S.; Gao, F. A quantum federated learning framework for classical clients. *Sci. China Phys. Mech. Astron.* **2024**, *67*, 250311. [CrossRef]
30. Lewis, M.; Glover, F. Quadratic unconstrained binary optimization problem preprocessing: Theory and empirical analysis. *Networks* **2017**, *70*, 79–97. [CrossRef]
31. Farhi, E.; Goldstone, J.; Gutmann, S. A quantum approximate optimization algorithm. *arXiv* **2014**, arXiv:1411.4028. [CrossRef]
32. Gambetta, J. Expanding the IBM Quantum Roadmap to Anticipate the Future of Quantum-Centric Supercomputing. 2022. Available online: https://www.ibm.com/quantum/blog/ibm-quantum-roadmap-2025 (accessed on 7 July 2024).
33. Bertero, F.; Bianchetti, M.; Marenco, J. Integer programming models for the routing and spectrum allocation problem. *Top* **2018**, *26*, 465–488. [CrossRef]
34. Talebi, S.; Alam, F.; Katib, I.; Khamis, M.; Salama, R.; Rouskas, G.N. Spectrum management techniques for elastic optical networks: A survey. *Opt. Switch. Netw.* **2014**, *13*, 34–48. [CrossRef]
35. Xu, L.; Huang, Y.C.; Xue, Y.; Hu, X. Deep Reinforcement Learning-Based Routing and Spectrum Assignment of EONs by Exploiting GCN and RNN for Feature Extraction. *J. Light. Technol.* **2022**, *40*, 4945–4955. [CrossRef]
36. Chen, J.; Huang, H.; Zhang, Z.; Wang, J. Deep Reinforcement Learning with Two-Stage Training Strategy for Practical Electric Vehicle Routing Problem with Time Windows. In Proceedings of the Parallel Problem Solving from Nature—PPSN XVII, Dortmund, Germany, 10–14 September 2022; Rudolph, G., Kononova, A.V., Aguirre, H., Kerschke, P., Ochoa, G., Tušar, T., Eds.; Springer: Cham, Switzerland, 2022; pp. 356–370. [CrossRef]
37. Coraci, D.; Brandi, S.; Capozzoli, A. Effective pre-training of a deep reinforcement learning agent by means of long short-term memory models for thermal energy management in buildings. *Energy Convers. Manag.* **2023**, *291*, 117303. [CrossRef]
38. Klinkowski, M.; Walkowiak, K. Routing and Spectrum Assignment in Spectrum Sliced Elastic Optical Path Network. *IEEE Commun. Lett.* **2011**, *15*, 884–886. [CrossRef]
39. Wang, R.; Mukherjee, B. Provisioning in Elastic Optical Networks with Non-Disruptive Defragmentation. *J. Light. Technol.* **2013**, *31*, 2491–2500. [CrossRef]
40. Zhang, Y.; Xin, J.; Li, X.; Huang, S. Overview on routing and resource allocation based machine learning in optical networks. *Opt. Fiber Technol.* **2020**, *60*, 102355. [CrossRef]
41. Montanez-Barrera, J.A.; Michielsen, K. Towards a universal QAOA protocol: Evidence of a scaling advantage in solving some combinatorial optimization problems. *arXiv* **2024**, arXiv:2405.09169 .
42. Blekos, K.; Brand, D.; Ceschini, A.; Chou, C.H.; Li, R.H.; Pandya, K.; Summer, A. A review on quantum approximate optimization algorithm and its variants. *Phys. Rep.* **2024**, *1068*, 1–66. [CrossRef]

Disclaimer/Publisher's Note: The statements, opinions and data contained in all publications are solely those of the individual author(s) and contributor(s) and not of MDPI and/or the editor(s). MDPI and/or the editor(s) disclaim responsibility for any injury to people or property resulting from any ideas, methods, instructions or products referred to in the content.